

Ill-conditioning in the virtual element method: Stabilizations and bases

Lorenzo Mascotto 

Faculty of Mathematics, University of Vienna, 1090 Vienna, Austria

Correspondence

Lorenzo Mascotto, Faculty of Mathematics, University of Vienna, 1090 Vienna, Austria.
Email: lorenzo.mascotto@univie.ac.at

In this article, we investigate the behavior of the condition number of the stiffness matrix resulting from the approximation of a 2D Poisson problem by means of the virtual element method. It turns out that ill-conditioning appears when considering high-order methods or in presence of “bad-shaped” (for instance nonuniformly star-shaped, with small edges...) sequences of polygons. We show that in order to improve such condition number one can modify the definition of the internal moments by choosing proper polynomial functions that are not the standard monomials. We also give numerical evidence that at least for a 2D problem, standard choices for the stabilization give similar results in terms of condition number.

KEYWORDS

virtual element methods, hp Galerkin methods, Ill-conditioning

1 | INTRODUCTION

The interest in numerical methods for the approximation of partial differential equations (PDEs in short) based on polytopical grids has grown in the last decade, due to the high flexibility that polygonal/polyhedral meshes allow. Among the other methods, we here recall only a short list including: mimetic finite differences [1, 2], discontinuous Galerkin-finite element method (DG-FEM) [3, 4], hybridizable and hybrid high-order methods [5, 6], weak Galerkin method [7], BEM-based FEM [8], and polygonal FEM [9].

An alternative approach is offered by the virtual element method (VEM in short), recently introduced in [10]. VEM are a generalization of the finite element method (FEM in short) enabling the employment of polytopal meshes and the possibility of building high-order methods. In addition to polynomials, local VE spaces consist of other functions instrumental for constructing global H^1 conforming approximation space; such functions are typically the solution to local PDEs and therefore

.....
This is an open access article under the terms of the Creative Commons Attribution License, which permits use, distribution and reproduction in any medium, provided the original work is properly cited.

© 2018 The Authors. Numerical Methods for Partial Differential Equations Published by Wiley Periodicals, Inc.

are not known explicitly in a closed-form. For this reason, VEM can be considered, for all practical purposes, Trefftz methods.

In VEM, the bilinear forms and the right-hand sides are not computed exactly due to the fact that the functions in VE spaces are not fully explicit. The VEM gospel states that such bilinear forms and right-hand sides are then approximated by means of discrete counterparts that are exactly computable only through the degrees of freedom and which scale like the continuous ones.

In a few years, thanks to high theoretical and practical flexibility of VEM, the size of associated literature has rapidly blown up. Among the other references, we recall the following: the p and hp version of the method [11–16], parabolic problems [17], Cahn-Hilliard, Stokes, Navier-Stokes and Helmholtz equations [18–22], linear and nonlinear elasticity problems [23–25], general elliptic problems [26], PDEs on surfaces [27], Domain Decomposition [28], application to discrete fracture networks [29], serendipity VEM [30], VEM on surfaces [27]. The implementation of the method is described in [31], whereas the basic principles of the 3D version of the method are the topic of [32, 33].

It was observed that the VEM stiffness matrix, similarly as FEM, can become ill-conditioned in various situations. This is the case for instance of the p and the hp version of VEM, as discussed in [11, 13], and in presence of “badly-shaped” (i.e., nonuniformly star-shaped, with small edges...) polygons, as discussed [34].

Among the possible reasons of this ill-conditioning we highlight two of them. The first one is related to the fact that in the VEM framework one does not use the exact bilinear form but an approximated one; the choice of the discrete bilinear form, and, in particular, of one of its two components, namely the stabilization of the method, may have an impact on the 3D version of VEM as observed in [33]. The second one is the choice of the basis. This is also the case for FEM, where the choice of the basis has an important role on the ill-conditioning of the system, see [35–37] and the references therein.

The aim of the present paper is to discuss various choices for both the discrete bilinear forms and the VE bases and check numerically that particular choices can cure the ill-conditioning which arises in high-order (or in presence of badly-shaped polygons) VEM.

In particular, we show that while the choice of the stabilization has not a deep impact on the ill-conditioning (at least for the 2D case, which is the focus of this article), a proper choice of the basis can actually improve the condition number of the stiffness matrix. However, it is worth to mention that in “standard” situations, that is, low-to-moderate order VEM and VEM applied to shape-regular decompositions, the standard VEM (e.g., the one described in [10]) is preferable, as the implementation of that version of the method turns out to be much simpler than those we are going to present in this article.

The outline of the article is the following. We firstly discuss the model problem and its VEM approximation in Section 2, while in Appendix A, we give a hint on the implementation details of the method using one of the new VEM basis. In Section 3, we present a number of numerical experiments comparing the behavior of the method when changing various stabilizations and VE bases.

In the remainder of the article, we adopt the standard notation for Sobolev spaces, see for example, [38, 39]. Given $\omega \subset \mathbb{R}^2$, we denote by $H^\ell(\omega)$, $\ell \in \mathbb{N}$, the Sobolev space of order ℓ over ω ; in the case $\ell = 0$, we set $H^0(\omega) = L^2(\omega)$, where $L^2(\omega)$ is the Lebesgue space of square integrable functions over ω . By $H_0^1(\Omega)$, we mean the Sobolev space H^1 of functions with zero trace. The Sobolev (semi)norms and inner products read, respectively:

$$|\cdot|_{\ell,\omega}, \quad \|\cdot\|_{\ell,\omega}, \quad (\cdot, \cdot)_{0,\omega}. \tag{1}$$

Further, given a Lipschitz domain ω with boundary Γ , we set \mathbf{n} the normal versor associated with Γ and $\partial_{\mathbf{n}}v = \nabla v \cdot \mathbf{n}$ the normal derivative of a sufficiently regular function v . By $\mathbb{P}_\ell(\omega)$, $\ell \in \mathbb{N}$, we denote the space of polynomials of degree ℓ over ω . Finally, given two positive quantities a and b ,

possibly depending on the discretization parameters h and p , we write $a \lesssim b$ if there exists a positive and parameter-independent constant c such that $a \leq cb$. Moreover, we write $a \approx b$ meaning that $a \lesssim b$ and $b \lesssim a$ simultaneously.

2 | THE VIRTUAL ELEMENT METHOD: DEFINITION, CHOICE OF THE STABILIZATION AND OF THE BASIS

Given $\Omega \subset \mathbb{R}^2$ a polygonal domain and $f \in L^2(\Omega)$, we consider the following 2D Poisson problem:

$$\begin{cases} \text{find } u \in V \text{ such that} \\ a(u, v) = (f, v)_{0, \Omega} \quad \forall v \in V \end{cases}, \quad \text{where } V := H_0^1(\Omega), \quad \text{and } a(\cdot, \cdot) := (\nabla \cdot, \nabla \cdot)_{0, \Omega}. \quad (2)$$

The outline of the present section is the following. In Section 2.1, we introduce a family of VEMs for the approximation of problem (2); here, both the stabilization, typical of VEM, and the choice of the basis of local VE space are kept at a very general level. Explicit choices for the stabilization are investigated in Section 2.2, whereas explicit choices for the local basis elements are the topic of Section 2.3. Finally, in Section 2.4, we highlight the influence of the choices of the stabilizations and of the local basis elements on the performances of the method.

2.1 | A family of VEM

Given Ω the computational domain of problem (2), we consider a family $\{\mathcal{T}_n\}_{n \in \mathbb{N}}$ of conforming polygonal decomposition of Ω , where by conforming we mean that, given an edge in the skeleton of the decomposition which does not lie on $\partial\Omega$, then it is an edge of *exactly* two polygons. We also fix $p \in \mathbb{N}$, which will represent the degree of accuracy of the method. We associate to each $K \in \mathcal{T}_n$ its diameter h_K and to decomposition \mathcal{T}_n its mesh size function $h = \max_{K \in \mathcal{T}_n} h_K$.

Standard regularity assumptions on decomposition \mathcal{T}_n that are usually required in VEM literature read:

- For every $K \in \mathcal{T}_n$, K is star-shaped (see [40]) with respect to a ball of radius greater or equal than γh_K , γ being a positive constant independent of the family of decompositions.
- For every $K \in \mathcal{T}_n$ and for every e edge of K , the length of e is greater or equal than γh_K , γ being the same constant introduced in assumption **(D1)**.

We point out that such assumptions can be relaxed, see [41].

We now define the local VE space on polygon $K \in \mathcal{T}_n$ following the standard definition given, for example, in [10]. Having set the space of piecewise continuous polynomials of degree p over ∂K :

$$\mathbb{B}_p(\partial K) := \{v_p \in \mathcal{C}^0(\partial K) | v_p|_e \in \mathbb{P}_p(e) \forall e \text{ edge of } K\}, \quad (3)$$

we introduce the local VE space as:

$$V_p(K) := \{v_p \in H^1(K) | v_p|_{\partial K} \in \mathbb{B}_p(\partial K), \Delta v_p \in \mathbb{P}_{p-2}(K)\}. \quad (4)$$

Space $V_p(K)$, which contains $\mathbb{P}_p(K)$, contains also other functions that in general are not known pointwise (hence, the name *virtual*), but which are added to polynomials in order to guarantee the possibility of building a H^1 conforming method over \mathcal{T}_n .

We associate to space $V_p(K)$ the following set of linear functionals. Given $v_p \in V_p(K)$:

- the point values of v_p at the vertices of K ;
- for every e edge of K , the point values of v_p at the $p - 1$ internal Gauß-Lobatto nodes of e ;
- the (scaled) internal moments:

$$\frac{1}{|K|} \int_K v_p q_\alpha, \tag{5}$$

where $\{q_\alpha\}_{\alpha=1}^{\dim(\mathbb{P}_{p-2}(K))}$ is any basis of $\mathbb{P}_{p-2}(K)$.

It was proven in [10] that this is a set of unisolvent degrees of freedom. Let N_{dof}^K be the number of such degrees of freedom, that is, the dimension of space $V_p(K)$. Henceforth, we denote by dof_i the i -th dof of space $V_p(K)$ and by:

$$\{\varphi_i\}_{i=1}^{N_{\text{dof}}^K} \tag{6}$$

the local canonical basis of space $V_p(K)$, which is dual to the set of degrees of freedom $\{\text{dof}_i\}_{i=1}^{\dim(V_p(K))}$, that is, the set of functions such that:

$$\text{dof}_i(\varphi_j) = \delta_{ij} = \begin{cases} 1 & \text{if } i = j \\ 0 & \text{otherwise} \end{cases} \quad \forall i, j = 1, \dots, N_{\text{dof}}^K. \tag{7}$$

Functions in the canonical basis associated with internal moments (5) are bubbles on element K as they vanish on the boundary.

It is fundamental to observe that the definition of space $V_p(K)$ is completely independent of the choice of polynomial basis $\{q_\alpha\}_{\alpha=1}^{\dim(\mathbb{P}_{p-2}(K))}$, which is, so far, *only* instrumental for the definition of the internal moments (5). Nonetheless, such a choice plays a crucial role in the behaviour of the condition number of the stiffness matrix of the method as discussed and shown in Section 3. In Subsection 2.3, we present many choices of basis $\{q_\alpha\}_{\alpha=0}^{p-2}$.

As already stressed, not all the functions in space $V_p(K)$ are known explicitly; nevertheless, it is possible to compute local H^1 and L^2 projections as shown in [10, 31] via the degrees of freedom above described. More precisely, it is possible to compute the following two operators.

The first one is the L^2 projector $\Pi_{p-2}^0 : V_p(K) \rightarrow \mathbb{P}_{p-2}(K)$ defined, for all $K \in \mathcal{T}_n$, by:

$$(q_{p-2}, \Pi_{p-2}^0 v_p - v_p)_{0,K} = 0 \quad \forall q_{p-2} \in \mathbb{P}_{p-2}(K), \forall v_p \in V_p(K), \tag{8}$$

which is clearly computable via internal moments (5).

The second one is a H^1 projector $\Pi_p^\nabla : V_p(K) \rightarrow \mathbb{P}_p(K)$ defined by:

$$\begin{cases} a^K(q_p, \Pi_p^\nabla v_p - v_p) = 0 \\ P_0(\Pi_p^\nabla v_p - v_p) = 0 \end{cases} \quad \forall q_p \in \mathbb{P}_p(K), \forall v_p \in V_p(K), \tag{9}$$

where $a^K(\cdot, \cdot) = (\nabla \cdot, \nabla \cdot)_{0,K}$ and where P is an operator which fixes the constant part of the energy projector Π_p^∇ defined as:

$$P_0(v_p) = \begin{cases} \frac{1}{N_K} \sum_{j=1}^{N_K} v_p(v_j) & \text{if } p = 1 \\ \int_K v_p & \text{otherwise} \end{cases} \quad \forall v_p \in V_p(K), \tag{10}$$

where $\{v_j\}_{j=1}^{N_K}$ is the set of vertices of polygon K . Operator Π_p^∇ is computable by means of the degrees of freedom, noting that:

$$a^K(q_p, v_p) = - \int_K \Delta q_p v_p + \int_{\partial K} \partial_n q_p v_p \quad \forall q_p \in \mathbb{P}_p(K), \forall v_p \in V_p(K)$$

and recalling that $v_p \in V_p(K)$.

At this point, we turn our attention to the computation of the local stiffness matrix and of the local right-hand side. In both cases, we cannot use their continuous counterparts as we do not know pointwise functions in space $V_p(K)$. Therefore, we follow the VEM gospel and we note that Pythagoras Theorem for Hilbert spaces asserts:

$$a^K(u_p, v_p) = a^K(\Pi_p^\nabla u_p, \Pi_p^\nabla v_p) + a^K((I - \Pi_p^\nabla)u_p, (I - \Pi_p^\nabla)v_p) \quad \forall u_p, v_p \in V_p(K). \tag{11}$$

If we split the local space $V_p(K)$ into a polynomial and a ‘‘pure virtual’’ part:

$$\begin{aligned} V_p(K) &= \{v_p \in V_p(K) | v_p \in \mathbb{P}_p(K)\} \oplus \{v_p \in V_p(K) | \Pi_p^\nabla v_p = 0\} \\ &= \mathbb{P}_p(K) \oplus \ker(\Pi_p^\nabla) =: V_{p,1}(K) \oplus V_{p,2}(K), \end{aligned} \tag{12}$$

then the first term on the right-hand side of (11) is identically zero on $V_{p,2}(K)$, while the second one annihilates on $V_{p,1}(K)$.

We point out that, given N_K the number of vertices of K , one has:

$$\begin{aligned} \dim(V_{p,1}(K)) &= \dim(\mathbb{P}_p(K)) = \frac{(p+1)(p+2)}{2}, \\ \dim(V_{p,2}(K)) &= \dim(V_p(K)) - \dim(V_{p,1}(K)) \\ &= N_K \cdot p + \frac{(p-1)p}{2} - \frac{(p+1)(p+2)}{2} = (N_K - 2)p - 1. \end{aligned} \tag{13}$$

This entails that the actual ‘‘pure virtual’’ part of space $V_p(K)$, that is, $\ker(\Pi_p^\nabla)$, is asymptotically smaller than its polynomial counterpart, if the number of vertices of K remains uniformly bounded. More precisely, $\dim(V_{p,2}(K)) \approx p$ whereas $\dim(V_{p,1}(K)) \approx p^2$.

We emphasize that the first term on the right-hand side of (11) is explicitly computable but the second one is not. For this reason, one substitutes:

$$a^K((I - \Pi_p^\nabla)u_p, (I - \Pi_p^\nabla)v_p) \Rightarrow S^K((I - \Pi_p^\nabla)u_p, (I - \Pi_p^\nabla)v_p),$$

where $S^K(\cdot, \cdot)$ is any bilinear form mimicking the continuous one, that is, $a^K(\cdot, \cdot)$ on $\ker(\Pi_p^\nabla) \times \ker(\Pi_p^\nabla)$. To have a well-posed method, we demand the following stability assumption on the bilinear form S^K :

$$c_*(p) |v_p|_{1,K}^2 \leq S^K(v_p, v_p) \leq c^*(p) |v_p|_{1,K}^2 \quad \forall v_p \in \ker(\Pi_p^\nabla), \tag{14}$$

where $c_*(p)$ and $c^*(p)$ are two positive constants possibly depending on p . Various possible stabilizations S^K are presented in Section 2.2.

By defining the local discrete bilinear form as:

$$a_p^K(u_p, v_p) = a^K(u_p, v_p) + S^K((I - \Pi_p^\nabla)u_p, (I - \Pi_p^\nabla)v_p) \quad \forall u_p, v_p \in V_p(K), \tag{15}$$

one can prove the following properties for $a_p^K(\cdot, \cdot)$:

(P1) p -consistency: for every $q_p \in \mathbb{P}_p(K)$ and for every $v_p \in V_p(K)$, the local bilinear form a_p^K satisfies:

$$a^K(q_p, v_p) = a_p^K(q_p, v_p); \tag{16}$$

(P2) stability: for every $v_p \in V_p(K)$, the local bilinear form a_p^K satisfies:

$$\alpha_*(p)|v_p|^2 \leq a_p^K(v_p, v_p) \leq \alpha^*(p)|v_p|^2, \tag{17}$$

where $\alpha_*(p) = \min(1, c_*(p))$ and $\alpha^*(p) = \max(1, c^*(p))$.

Regarding the local discrete right-hand side, we set:

$$\langle f_n, v_p \rangle_K := \begin{cases} \int_K (f \int_{\partial K} v_p) & \text{if } p = 1 \\ \int_K f \Pi_{p-2}^0 v_p & \text{otherwise} \end{cases} \quad \forall v_p \in V_p(K). \tag{18}$$

At this point, we are able to define the global VE space, which is obtained by a standard dof coupling of the local spaces:

$$V_p := \{v_p \in V \cap C^0(\overline{\Omega}) | v_p|_K \in V_p(K) \forall K \in \mathcal{T}_n\} \tag{19}$$

and the discrete global bilinear form and right-hand side:

$$a_p(u_p, v_p) = \sum_{K \in \mathcal{T}_n} a_p^K(u_p, v_p), \quad \langle f_n, v_p \rangle = \sum_{K \in \mathcal{T}_n} \langle f_n, v_p \rangle_K \quad \forall u_p, v_p \in V_p. \tag{20}$$

We now define a family of VEMs depending on the choice of the local stabilization S^K defined in (14):

$$\begin{cases} \text{find } u_p \in V_p \text{ such that} \\ a_p(u_p, v_p) = \langle f_n, v_p \rangle \quad \forall v_p \in V_p \end{cases} . \tag{21}$$

Property **(P1)** guarantees that the patch test is satisfied by **(P1)** solution with a polynomial degree smaller than or equal to p (the polynomial accuracy of the method).

Conversely, property **(P2)** implies the coercivity and the continuity of the discrete bilinear form and thus the well-posedness of methods (21). It is worth to stress that the coercivity and continuity constants may depend on p , owing to (17).

Let us set the H^1 broken Sobolev seminorm associated with decomposition \mathcal{T}_n as:

$$|\cdot|_{1, \mathcal{T}_n; \Omega}^2 = \sum_{K \in \mathcal{T}_n} |\cdot|_{1, K}^2. \tag{22}$$

and let us set $S^{p,-1}(\Omega, \mathcal{T}_n)$ the space of piecewise discontinuous polynomials of degree p over decomposition \mathcal{T}_n .

Having properties **(P1)** and **(P2)**, one can prove as in [11, 12] an abstract error analysis result. Given u and u_p the solutions to (2) and (21), respectively, the following holds true:

$$|u - u_p|_{1,\Omega} \lesssim \frac{\alpha^*(p)}{\alpha_*(p)} \{|u - u_\pi|_{1,\mathcal{T}_n;\Omega} + |u - u_I|_{1,\Omega} + \mathcal{F}_n\} \quad \forall u_\pi \in S^{p,-1}(\Omega, \mathcal{T}_n), \forall u_I \in V_p, \quad (23)$$

where \mathcal{F}_n is the smallest positive constant such that

$$|(f, v_p)_{0,\Omega} - \langle f_n, v_p \rangle| \leq \mathcal{F}_n |v_p|_{1,\Omega} \quad \forall v_p \in V_p.$$

Thus, being able to study the convergence of the method is equivalent to being able to prove best approximation results by piecewise discontinuous polynomials in $S^{p,-1}(\Omega, \mathcal{T}_n)$ and by functions in V_p , the global VE space defined in (19).

In [11, 12], it was proven that for any u , solution to (2), in $H^{k+1}(\Omega)$, the following hp a priori estimate holds true:

$$|u - u_p|_{1,\Omega} \lesssim \frac{\alpha^*(p)}{\alpha_*(p)} \frac{h^{\min(p,k)}}{p^k} |u|_{k+1,\Omega} \quad (24)$$

and that for u analytic on a proper extension of Ω , the following pure p approximation result holds true:

$$|u - u_p|_{1,\Omega} \lesssim \frac{\alpha^*(p)}{\alpha_*(p)} \exp(-bp), \quad (25)$$

where b is a positive constant independent of the discretization parameters.

The dependence on p of the pollution factor $\frac{\alpha^*(p)}{\alpha_*(p)}$ is clearly an issue of extreme importance in the p analysis of the method. The following crude upper bound:

$$\frac{\alpha^*(p)}{\alpha_*(p)} \lesssim p^5,$$

using a particular stabilization, was proved in [12, Theorem 2]. However, numerical experiments on different stabilizations highlight that the dependence on p is much milder; typically, even on nonconvex and nonstar-shaped polygons, one has $\frac{\alpha^*(p)}{\alpha_*(p)} \lesssim p^\beta$, for some $\beta \in (0, 1)$; see [12, 11].

It is worth to stress that such algebraic dependence on the degree of accuracy does not affect the exponential convergence (25) when approximating analytic solution. Importantly, it is possible to get rid of the dependence on the pollution factor also when approximating solutions presenting corner singularities, using the hp version of the method; see [12].

2.2 | Choices for the stabilization

Here, we address the issue of choosing a proper stabilization S^K (14) for method (21). In particular, we define four possible stabilizations which can be found in literature and we discuss their properties. We recall that N_{dof}^K is the number of dofs of local space $V_p(K)$.

The first stabilization that we present is:

$$S_1^K(u_p, v_p) = \sum_{i=1}^{N_{\text{dof}}^K} \text{dof}_i(u_p) \text{dof}_i(v_p), \tag{26}$$

which can be regarded as the ‘‘standard’’ stabilization of VEM. It was firstly introduced in [10] and it can be proved that, for a fixed degree of accuracy p , S_1^K scales like the H^1 seminorm. We highlight that this holds true only in two dimension; for a three dimensional problem one should put a proper scaling factor in front of S_1^K , see [33, 32]. The advantage of picking S_1^K as a stabilization is that its implementation is extremely easy.

If one takes into account also variable p , then one has to prove the dependence on p of the stability constant in (14). This was done in [12], where the authors introduced the following *computable* stabilization:

$$S_2^K(u_p, v_p) = \frac{p}{h_K} (u_p, v_p)_{0,\partial K} + \frac{p^2}{h_K^2} (\Pi_{p-2}^0 u_p, \Pi_{p-2}^0 v_p)_{0,K}. \tag{27}$$

At the current theoretical level, the stabilization constants $c_*(p)$ and $c^*(p)$ which appear in (14) have a dreadful dependence on p ; nonetheless, at the practical level, it was observed in [12] an extremely mild dependence on p of $c_*(p)$ and $c^*(p)$.

Next, we recall another stabilization which was introduced in [33]. If we denote by \mathbf{K}_C^K the consistency part of the local stiffness matrix, that is, the matrix counterpart of the first term on the right-hand side of (15), then we can define a stabilization S_3^K through its matrix representation \mathbf{S}_3^K associated with the second term on the right-hand side of (15) as follows. \mathbf{S}_3^K is a diagonal matrix, whose i -th entry is given by:

$$(\mathbf{S}_3^K)_{i,i} = \max(1, (\mathbf{K}_C^K)_{i,i}). \tag{28}$$

For the sake of clarity, the complete local stiffness matrix \mathbf{K}_n^K reads:

$$\mathbf{K}_p^K = \mathbf{K}_C^K + \mathbf{K}_{S_3}^K = \mathbf{K}_C^K + (\mathbf{Id} - \mathbf{\Pi}^\nabla)^T \cdot \mathbf{S}_3^K \cdot (\mathbf{Id} - \mathbf{\Pi}^\nabla),$$

where $\mathbf{\Pi}^\nabla$ is the matrix representing the action of operator Π_p^∇ and \mathbf{S}_3^K is defined in (28).

In [33], numerical experiments, along with a heuristic motivation, show that choice (28) entails a better behaviour of the method for high p , when approximating a 3D Poisson problem.

Finally, we also consider a fourth stabilization. Let $N_{\text{dof}}^{\text{bndr}}$ be the number of boundary degrees of freedom of $V_p(K)$. Then, we set:

$$S_4^K(u_p, v_p) = \sum_{i=1}^{N_{\text{dof}}^{\text{bndr}}} \text{dof}_i(u_p) \text{dof}_i(v_p), \tag{29}$$

which is basically stabilization S_1^K without the contribution of internal dofs.

We point out that other choices of stabilization can be found in literature, but we prefer to investigate the four presented here in order to avoid an overwhelming set of numerical experiments.

We also emphasize that the first three stabilizations above hinge on the choice of the polynomial basis dual to internal moments (5).

2.3 | Choices for the basis

In this section, we discuss three possible choices of the local VE basis. More precisely, we consider internal moments (5) taken with respect to three different polynomial bases $\{q_\alpha^i\}_{\alpha=1}^{\dim(\mathbb{P}_{p-2}(K))}$, $i = 1, 2, 3$, of $\mathbb{P}_{p-2}(K)$, thus modifying the definition of the VE bubble functions.

The hope is that a proper choice of the polynomial basis dual to internal moments (5), and therefore, of internal VEM basis elements, entails a better conditioning for the stiffness matrix.

Henceforth, we will use, with an abuse of notation, the natural bijection $\mathbb{N}^2 \leftrightarrow \mathbb{N}_0$ given by:

$$(0, 0) \leftrightarrow 1, \quad (1, 0) \leftrightarrow 2, \quad (0, 1) \leftrightarrow 3, \quad (2, 0) \leftrightarrow 4, \quad (1, 1) \leftrightarrow 5, \quad (0, 2) \leftrightarrow 6, \quad \dots \quad (30)$$

We will also write occasionally:

$$\{q_\alpha^i\}_{|\alpha|=0}^{p-2} \quad \text{instead of} \quad \{q_\alpha^i\}_{\alpha=1}^{\dim(\mathbb{P}_{p-2}(K))}, \quad \text{for } i = 1, 2, 3.$$

The first choice of the polynomial basis is the ‘‘standard’’ one, that is, the one which is used in the majority of VEM literature, since, at the implementation level, is the most convenient. Given $\mathbf{x}_K = (x_K, y_K)$ the barycenter of K , we set:

$$q_\alpha^1(\mathbf{x}) = \left(\frac{\mathbf{x} - \mathbf{x}_K}{h_K}\right)^\alpha = \left(\frac{x - x_K}{h_K}\right)^{\alpha_1} \left(\frac{y - y_K}{h_K}\right)^{\alpha_2} \quad \forall \alpha = (\alpha_1, \alpha_2) \in \mathbb{N}^2, \quad |\alpha| = 0, \dots, p - 2. \quad (31)$$

Although choice (31) is very suitable from the computational point of view, it has bad effects on the condition number of the stiffness matrix for high local degrees of accuracy p , see [11], and in presence of badly-shaped polygons, see [34] and the references therein.

For this reason, we suggest two possible modifications which rely on orthogonalizing processes of $\{q_\alpha^1\}_{|\alpha|=0}^{p-2}$ with respect to the L^2 norm on polygon K .

The first modification, which allows to construct an $L^2(K)$ orthonormal basis $\{q_\alpha^2\}_{|\alpha|=0}^{p-2}$, is based on the stable Gram-Schmidt orthonormalization process presented in [42]. We point out that basis $\{q_\alpha^2\}_{|\alpha|=0}^{p-2}$ was firstly introduced in the context of p -VEM multigrid algorithm for the construction of the multigrid scheme, see [13].

While the implementation of VEM with basis $\{q_\alpha^1\}_{|\alpha|=0}^{p-2}$ is well-known (see [31]), no details were given in [13] for the implementation of the method using basis $\{q_\alpha^2\}_{|\alpha|=0}^{p-2}$. Therefore, we address this issue in Appendix A.

The third choice of the polynomial basis is slightly inspired by an orthonormalizing procedure used in [34]. To present the third basis $\{q_\alpha^3\}_{|\alpha|=0}^{p-2}$, we set matrix:

$$\mathbf{H}_{\alpha,\beta} = (q_\alpha^1, q_\beta^1)_{0,K} \quad \forall \alpha, \beta \in \mathbb{N}^2, \quad |\alpha|, |\beta| = 0, \dots, p - 2.$$

Given $n_\ell = \dim(\mathbb{P}_\ell(K))$, we fix $q_\alpha^3 = q_\alpha^1$ if $\alpha = 0$ and we decompose matrix \mathbf{H} into blocks as:

$$\mathbf{H} = \begin{matrix} & & 1 & n_{p-2} - 1 \\ & 1 & \begin{pmatrix} \mathbf{H}_{1,1} & \mathbf{H}_{1,2} \\ \mathbf{H}_{2,1} & \mathbf{H}_{2,2} \end{pmatrix} \\ n_{p-2} - 1 & & & \end{matrix}$$

we diagonalize matrix $\mathbf{H}_{2,2}$ and we get:

$$\mathbf{V}' \cdot \mathbf{H}_{2,2} \cdot \mathbf{V} = \mathbf{D} \Rightarrow (\mathbf{V} \cdot \mathbf{D}^{-\frac{1}{2}})' \cdot \mathbf{H}_{2,2} \cdot (\mathbf{V} \cdot \mathbf{D}^{-\frac{1}{2}}) = \mathbf{Id}.$$

This entails that matrix $\mathbf{V} \cdot \mathbf{D}^{-\frac{1}{2}}$ contains the coefficients which orthonormalize $\{q_\alpha^1\}_{|\alpha|=1}^{p-2}$, the monomial basis of $\mathbb{P}_{p-2}(K)/\mathbb{R}$. Therefore, one has:

$$q_\alpha^3(\mathbf{x}) = \begin{cases} q_\alpha^1 & \text{if } |\alpha| = 0 \\ \sum_{|\beta|=1}^{p-2} (\mathbf{V} \cdot \mathbf{D}^{-\frac{1}{2}})_{\alpha,\beta}^t q_\beta^1(\mathbf{x}) & \text{if } |\alpha| = 1, \dots, p-2 \end{cases} \quad (32)$$

Importantly, the basis in (32) is not completely orthogonal, as the orthogonalization process is performed on the block $\mathbf{H}_{2,2}$ only.

It is worth to stress that here the orthonormalizing process is performed with a different target with respect to what done in [34]; in fact, there, the method is built using the canonical bases computed taking moments with respect to scaled monomials $\{q_\alpha^1\}_{|\alpha|=0}^{p-2}$, whereas the construction of the local VE matrices is based on the usage of a polynomial basis similar to the basis $\{q_\alpha^3\}_{|\alpha|=0}^{p-2}$, obtained more precisely by diagonalizing the complete matrix \mathbf{H} instead of $\mathbf{H}_{2,2}$. Here, we define in addition internal moments with respect to basis $\{q_\alpha^3\}_{|\alpha|=0}^{p-2}$.

The implementation issues regarding this new basis are not explicated in this article, but are similar to those of basis $\{q_\alpha^2\}_{|\alpha|=0}^{p-2}$, which are shown in Appendix A.

In summary, we presented three choices for the polynomial basis dual to internal moments (5). One is of easy implementation, but it may be the cause of a high condition number for the stiffness matrix when using high-order methods or in presence of “badly-shaped” polygons. The other two bases are obtained by two distinct orthonormalization processes; their performances with respect to the condition number are investigated in Section 3. What we can anticipate is that they outclass the performances of their counterpart using the standard basis $\{q_\alpha^1\}_{|\alpha|=0}^{p-2}$ in the two situations above mentioned.

A *heuristic* reason for this fact is the following. If, for each element K , the local virtual element space $V_p(K)$ were a space consisting of polynomials only, then picking internal moments (5) with respect to an $L^2(K)$ orthonormal polynomial basis would automatically entail that the local canonical basis is made of polynomials and contain a subset of $L^2(K)$ orthonormal polynomials spanning $\mathbb{P}_{p-2}(K)$; it is well-known in the theory of Spectral Elements, see for example, [43, 44], that using L^2 orthonormal canonical basis damp the condition number of the stiffness matrix when increasing the polynomial degree.

Nonetheless, local virtual element spaces does not contain polynomials only, but also other functions needed for prescribing H^1 conformity. As stated in (13), the dimension of the subspace of nonpolynomial functions is, in terms of the degree of accuracy, asymptotically smaller than the dimension of the subspace of polynomial functions. Therefore, *in a very rough sense*, using L^2 orthonormal polynomials in the definition of internal moments entails a sort of *partial “orthonormalization”* of the local canonical basis.

Before concluding this section, we associate to bases $\{q_\alpha^i\}_{|\alpha|=0}^{p-2}$ the sets of dofs $\{\text{dof}_j^i\}_{j=1}^{N_{\text{dof}}^K}$ and the canonical bases $\{\varphi_j^i\}_{j=1}^{N_{\text{dof}}^K}$, for all $i = 1, 2, 3$. This notation will be instrumental in Appendix A.

2.4 | Stabilizations and bases: the effects on the method

Having presented in the two foregoing sections various choices of stabilizations and canonical bases, we want here to highlight the effects of such choices on the method and on the ill-conditioning of the stiffness matrix.

2.4.1 | Stabilization

The choice of the stabilization has two effects. The first one is related to the convergence of the method since nonproperly tailored choices of the stabilization automatically entail higher pollution factor $\frac{\alpha^*(p)}{\alpha_*(p)}$,

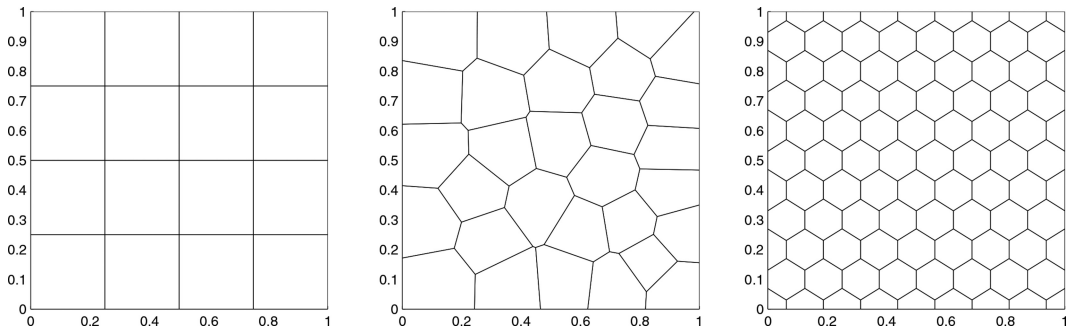


FIGURE 1 Left: square mesh. Center: Voronoi-Lloyd mesh. Right: regular-hexagonal mesh

see (25) and especially (24). Second, as the stabilization appears in the discrete bilinear form of the method, see (15), there is also an effect on the condition number of the stiffness matrix.

2.4.2 | Canonical basis

The choice of the canonical basis has also two effects. First, it has an impact on the condition number of the global stiffness matrix, simply because by changing the basis automatically the entries of the stiffness matrix modify. Second, by picking different canonical bases, one also changes the definition of the stabilization; as an example, if we fix stabilization S_1^K defined in (26) and we apply it to functions in the virtual element space, then we get in general different values, as the definition of the internal degrees of freedom vary depending on the choice of the basis; in particular, one also modify the behaviour of the pollution factor $\frac{\alpha^*(p)}{\alpha_*(p)}$.

3 | NUMERICAL RESULTS

In this section, we present some numerical experiments in which we compare the performances of the stabilizations and polynomial bases introduced in Sections 2.2 and 2.3, respectively.

More precisely, we investigate the behaviour and the related effects of the condition number in two critical situations.

In Section 3.1, we investigate the behavior of the condition number of the p version of VEM and the effects on the linear solver used for the resolution of the associated linear system. We are also interested in the behavior of the condition number when varying the stabilization and the polynomial basis dual to internal moments (5) in presence of a sequence of “bad shaped” polygons (collapsing bulk, collapsing edges...); this is probed in Sections 3.2 and 3.3. The condition number is computed as the ratio between the maximum and the minimum (nonzero) eigenvalue of the stiffness matrix.

3.1 | Numerical results: the p version of VEM

Let us consider the three meshes depicted in Figure 1. We investigate in this section the behaviour of the condition number of the stiffness matrix associated with method (21) by keeping fixed the meshes of Figure 1 and by increasing p . For the purpose, we modify the choice of the stabilization and the choice of the polynomial basis dual to internal moments (5).

In Figure 2, we depict the behaviour of the condition number by fixing the stabilization to be S_1^K presented in (26) and we consider the three polynomial bases introduced in Section 2.3. For all the

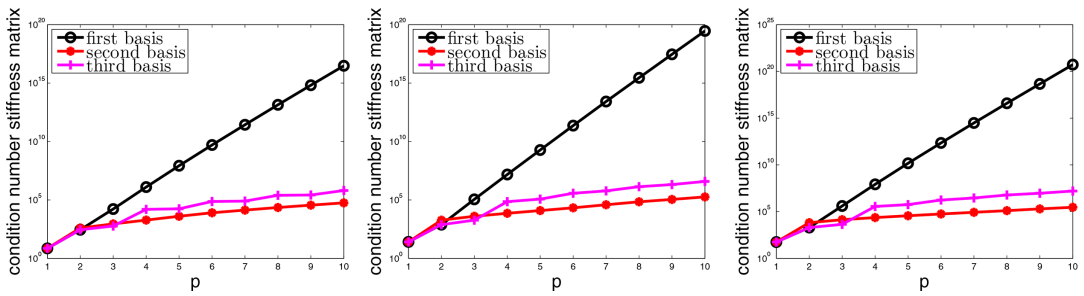


FIGURE 2 Condition number of the VEM stiffness matrix in terms of p . The stabilization is fixed and equal to S_1^K (26). We compare the behaviour in terms of the three polynomial bases presented in Section 2.3. Left: square mesh. Center: Voronoi-Lloyd mesh. Right: regular-hexagonal mesh [Color figure can be viewed at wileyonlinelibrary.com]

three meshes, the basis $\{q_\alpha^2\}_{|\alpha|=0}^{p-2}$ shows the best performances, whereas the standard monomial basis $\{q_\alpha^1\}_{|\alpha|=0}^{p-2}$ shows the worst results.

From Figure 2, it is also clear that basis $\{q_\alpha^1\}_{|\alpha|=0}^{p-2}$ entails an *exponential* growth of the condition number in terms of p .

Furthermore, using $\{q_\alpha^i\}_{|\alpha|=0}^{p-2}, i = 2, 3$, suggests instead an algebraic growth of the condition number in terms of p . A polynomial fitting yields:

$$\text{cond}(\mathbf{K}_p) \approx ap^b \quad \text{with } a = \begin{cases} 130.4 & \text{if } i = 2 \\ 131.7 & \text{if } i = 3 \end{cases}, \quad b = \begin{cases} 3.344 & \text{if } i = 2 \\ 3.371 & \text{if } i = 3 \end{cases}. \quad (33)$$

This behavior is extremely interesting since it is well-known, see for example, [43], that the growth in terms of p of the condition number in triangular Spectral Elements with nodal bases is of the following sort:

$$\text{cond}(\mathbf{K}_p) \approx ap^b \quad \text{with } b = 4, \quad \text{for some } a > 0. \quad (34)$$

We want now to understand how much the ill-conditioning pollutes the convergence of the error:

$$|u - \Pi_p^\nabla u_p|_{1, \mathcal{T}_n} := \sqrt{\sum_{K \in \mathcal{T}_n} |u - \Pi_p^\nabla u_p|_{1, K}^2}, \quad (35)$$

where we recall that u is the solution to (2) and u_p is its VEM approximation.

For the purpose, we consider a test case with analytic solution:

$$u(x, y) = \sin(\pi x) \sin(\pi y), \quad (36)$$

for which we know that the method converges exponentially, see (25). In Figure 3, we compare the errors (35) using the three meshes in Figure 1 (always using S_1^K (26) as a stabilization) and comparing the three bases $\{q_\alpha^i\}_{|\alpha|=0}^{p-2}, i = 1, 2, 3$. We observe that, due to the ill-conditioning of basis $\{q_\alpha^1\}_{|\alpha|=0}^{p-2}$ for high values of p , the linear solver of the system (namely the one associated with the `\` command of MATLAB) does not work properly. For this reason, we highly recommend to use basis $\{q_\alpha^2\}_{|\alpha|=0}^{p-2}$ in lieu of basis $\{q_\alpha^1\}_{|\alpha|=0}^{p-2}$ when approximating with high-order VEM.

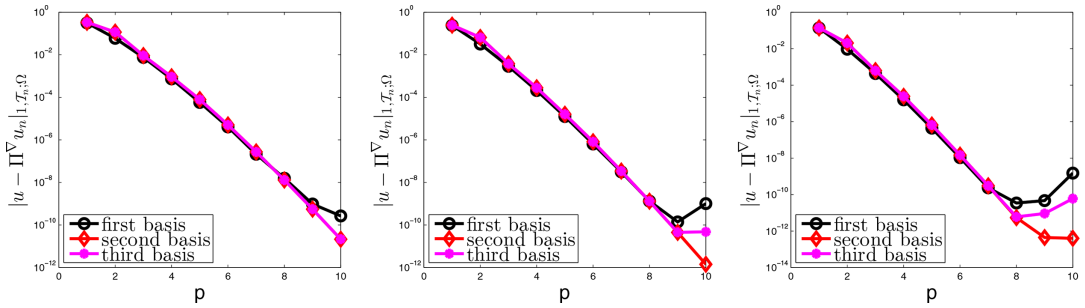


FIGURE 3 Error $|u - \Pi_p^\nabla u_p|_{1, \mathcal{T}_n}$ with exact solution given in (36). The stabilization is fixed and equal to S_1^K (26). We compare the behavior in terms of the three polynomial bases presented in Section 2.3. Left: square mesh. Center: Voronoi-Lloyd mesh. Right: regular-hexagonal mesh [Color figure can be viewed at wileyonlinelibrary.com]

To understand better “how much the (linear) solver fails” when solving the system arising from (21), we consider as an exact solution:

$$u(x, y) = 1 - x - y, \tag{37}$$

which, owing to polynomial consistency assumption (16), should be approximated exactly by the VEM.

In exact-arithmetic one would expect the error (35) to vanish, while in floating-point arithmetic the error is not zero but grows along with the condition number of the stiffness matrix.

In Figure 4, we compare error (35) using the three meshes in Figure 1, using S_1^K (26) as a stabilization and the three bases $\{q_\alpha^i\}_{|\alpha|=0}^{p-2}$, $i = 1, 2, 3$. The behaviour of basis $\{q_\alpha^2\}_{|\alpha|=0}^{p-2}$ is again superior to the other two bases. More precisely, using basis $\{q_\alpha^1\}_{|\alpha|=0}^{p-2}$ has a large effect on the error for high degrees of accuracy p .

To conclude this section, we present in Figure 5 a numerical test where we fix the polynomial basis dual to the internal moments (5) to be $\{q_\alpha^2\}_{|\alpha|=0}^{p-2}$ and we consider the four different stabilizations of Section 2.2. The stabilizations, as in the case of “bad” geometrical deformation presented in Section 3.2, have almost the same impact on the condition number (stabilization S_2^K seems to perform slightly worse than the other stabilizations).

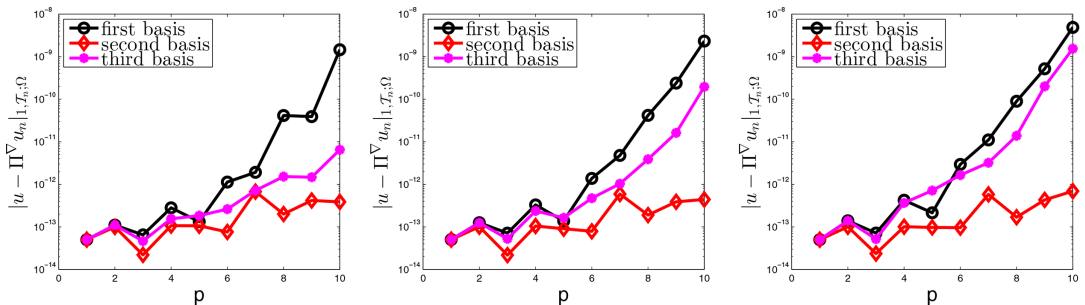


FIGURE 4 Error $|u - \Pi_p^\nabla u_p|_{1, \mathcal{T}_n}$ with exact solution given in (37). The stabilization is fixed and equal to S_1^K (26). We compare the behaviour in terms of the three polynomial bases presented in Section 2.3. Left: square mesh. Center: Voronoi-Lloyd mesh. Right: regular-hexagonal mesh [Color figure can be viewed at wileyonlinelibrary.com]

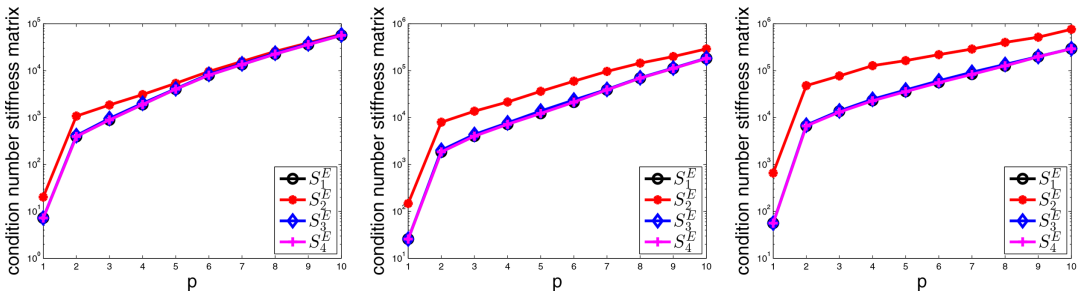


FIGURE 5 Condition numbers of the VEM stiffness matrix in terms of p on the three meshes depicted in Figure 1. The polynomial basis dual to internal moments (5) is $\{q_\alpha^2\}_{|\alpha|=0}^{p-2}$. We compare the behaviour in terms of the stabilizations presented in Section 2.2. Left: square mesh. Center: Voronoi-Lloyd mesh. Right: regular-hexagonal mesh [Color figure can be viewed at wileyonlinelibrary.com]

3.2 | Numerical results: collapsing polygons

It is also interesting to understand which is the impact of the choice of the stabilization and of the polynomial basis dual to internal moments (5) in presence of a sequence of “bad shaped” polygons (i.e., with collapsing bulk) on the condition number of the local stiffness matrix. In this way, we also test the robustness of the method when assumption **(D1)** is not valid.

For the purpose, we here present a quite limited and preliminary study. More precisely, we consider $\{K_i\}_{i \in \mathbb{N}}$, sequence of “collapsing” hexagons, as those depicted in Figure 6. In particular, the coordinates of K_i , the i -th element, are:

$$\begin{aligned} \mathbf{A}_i &= (1, 0), & \mathbf{B}_i &= (2, 2^{-i+1}), & \mathbf{C}_i &= (1, 2^{-i+2}), & \mathbf{D}_i &= (0, 2^{-i+1}), \\ \mathbf{E}_i &= (-1, 2^{-i+1}), & \mathbf{F}_i &= (0, 0). \end{aligned} \tag{38}$$

Needless to say, sequence K_i does not satisfy the star-shapedness assumption **(D1)**.

In Figure 7, we depict the behaviour of the condition number of the local stiffness matrix in terms of i , parameter used in the definition of the coordinates (38) of the pentagons K_i . In particular, we compare such behaviour employing the three bases $\{q_\alpha^i\}_{|\alpha|=0}^{p-2}$, $i = 1, 2, 3$, discussed in Section 2.3 and choosing $p = 3$ and $p = 6$, respectively. The stabilization is fixed to be S_4^K defined in (26). From Figure 7, we deduce that the standard choice for the polynomial basis (31) leads to a dramatic growth of the condition number. It turns out that the safest choice, in terms of ill-conditioning, is the one associated with basis $\{q_\alpha^2\}_{|\alpha|=0}^{p-2}$, which we recall is obtained by an orthonormalization of the standard monomial basis $\{q_\alpha^1\}_{|\alpha|=0}^{p-2}$ via a stable Gram-Schmidt process. Basis $\{q_\alpha^3\}_{|\alpha|=0}^{p-2}$, although behaves much better than the monomial basis, is not as good as $\{q_\alpha^2\}_{|\alpha|=0}^{p-2}$.

Next, in Figure 8, we compare the condition number of the stiffness matrix by fixing $p = 6$ and the polynomial basis $\{q_\alpha^2\}_{|\alpha|=0}^{p-2}$, which, from the previous tests, seems to be the best for the conditioning

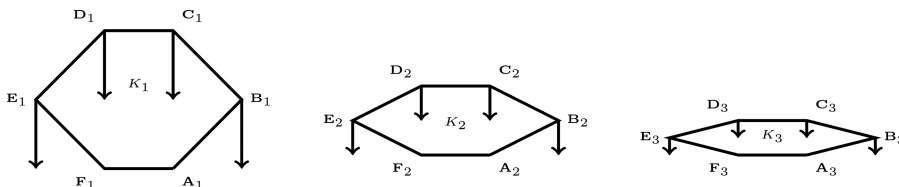


FIGURE 6 First three elements of sequence $\{K_i\}_{i \in \mathbb{N}}$ of hexagons with collapsing bulk

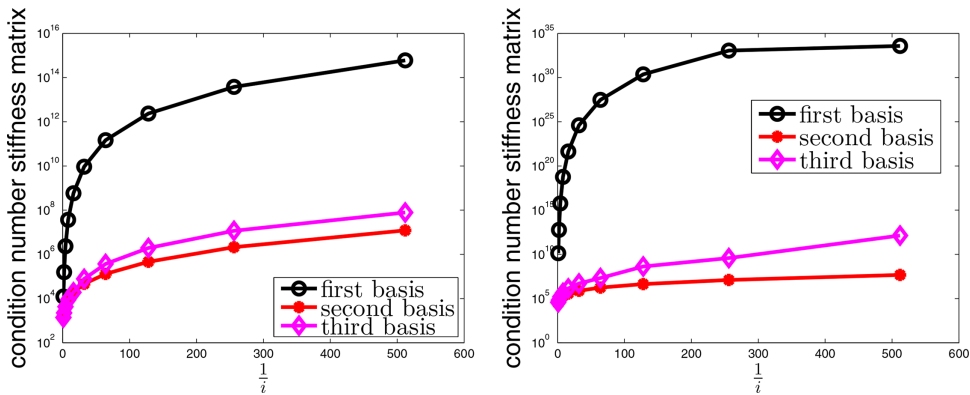


FIGURE 7 Condition numbers of the local VEM stiffness matrix on the sequence of hexagons depicted in Figure 6 in dependence of i , parameter used in the definition of the coordinates (38) of the pentagons K_i . The stabilization is fixed and equal to S_1^K (26). We compare the behaviour in terms of the three polynomial bases presented in Section 2.3. Left: $p=3$. Right: $p=6$ [Color figure can be viewed at wileyonlinelibrary.com]

of VEM, and by modifying the choice of the stabilizations; more precisely, we will consider the four stabilization discussed in Section 2.2. We deduce from Figure 8 that the choice of the stabilization does not have evident effects on the condition number, at least for the presented tests.

As a byproduct, in Figure 9, we consider a comparison between the four stabilizations by employing the standard monomial basis $\{q_\alpha^1\}_{|\alpha|=0}^{p-2}$ as dual basis for internal moments (5). Again, we assume $p = 6$.

3.3 | Numerical results: hanging nodes

As a final set of numerical results, we study the behavior of the condition number of the stiffness matrix using various bases and stabilizations in presence of hanging nodes collapsing on a vertex, checking thus the robustness of the method when assumption (D2) is not fulfilled.

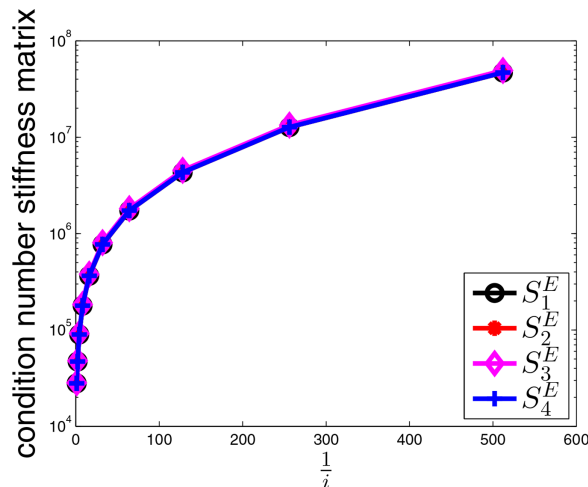


FIGURE 8 Condition numbers of the local VEM stiffness matrix on the sequence of hexagons depicted in Figure 6 in dependence of i , parameter used in the definition of the coordinates (38) of sequence $\{K_i\}_{i \in \mathbb{N}}$. The polynomial basis, dual to the internal moments (5) is fixed to be $\{q_\alpha^2\}_{|\alpha|=0}^{p-2}$. We compare the behavior in terms of the four stabilizations presented in Section 2.2. The degree of accuracy is $p=6$ [Color figure can be viewed at wileyonlinelibrary.com]

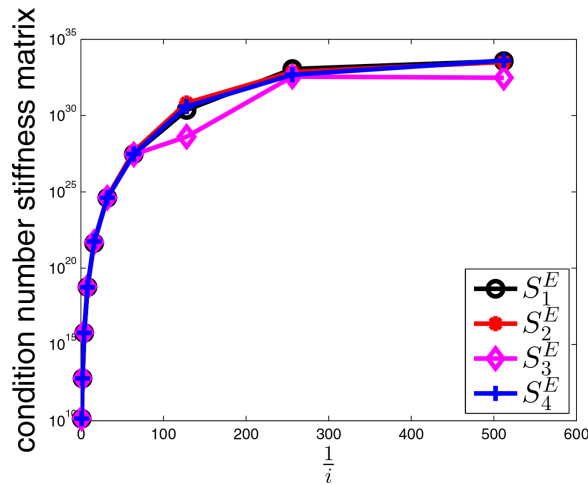


FIGURE 9 Condition numbers of the local VEM stiffness matrix on the sequence of hexagons depicted in Figure 6 in dependence of i , parameter used in the definition of the coordinates (38) of sequence $\{K_i\}_{i \in \mathbb{N}}$. The polynomial basis, dual to the internal moments (5) is fixed to be $\{q_\alpha^1\}_{|\alpha|=0}^{p-2}$. We compare the behavior in terms of the four stabilizations presented in Section 2.2. The degree of accuracy is $p=6$ [Color figure can be viewed at wileyonlinelibrary.com]

Again, we present here only a quite limited and preliminary study. In particular, we present a sequence of “squared pentagons,” that is a sequence of squares with a hanging node on a prescribed edge. More precisely, see Figure 10, we consider a sequence $\{K_i\}_{i \in \mathbb{N}}$ such that each $K_i, i \in \mathbb{N}$, has the following set of coordinates:

$$A_i = (1, 0), \quad B_i = (1, 1), \quad C_i = (2^{-i}, 1), \quad D_i = (0, 1), \quad E_i = (0, 0), i \in \mathbb{N}. \quad (39)$$

In Figure 11, we depict the behavior of the condition number of the local stiffness matrix in terms of i , parameter used in the definition of the coordinates (39) of the pentagons K_i . In particular, we compare such behavior using the three bases $\{q_\alpha^i\}_{|\alpha|=0}^{p-2}, i = 1, 2, 3$, discussed in Section 2.3 and choosing $p = 3$ and $p = 6$, respectively. The stabilization is fixed to be S_1^K defined in (26). The condition number is almost independent of parameter i for all choices of the canonical basis. This is not surprising since the bulk of the elements in the sequence remains the same for all i . However, when employing basis $\{q_\alpha^1\}_{|\alpha|=0}^{p-2}$, the condition number is higher.

Mimicking what done in Section 3.2, we compare in Figures 12 and 13 the condition number of the stiffness matrix by fixing $p = 6$ and the polynomial bases $\{q_\alpha^2\}_{|\alpha|=0}^{p-2}$ and $\{q_\alpha^1\}_{|\alpha|=0}^{p-2}$, respectively, and by considering the four stabilization discussed in Section 2.2.

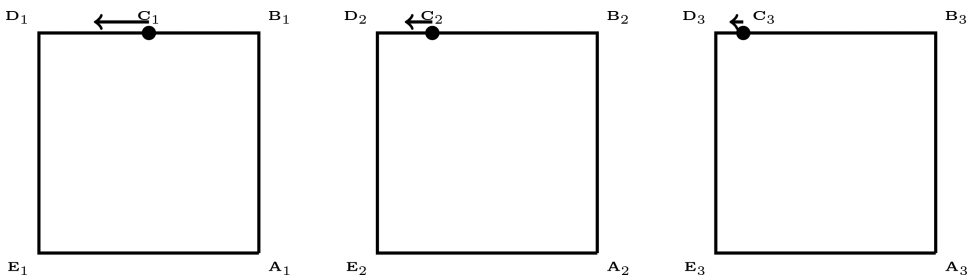


FIGURE 10 First three elements of sequence $\{K_i\}_{i \in \mathbb{N}}$ with hanging node collapsing on a vertex

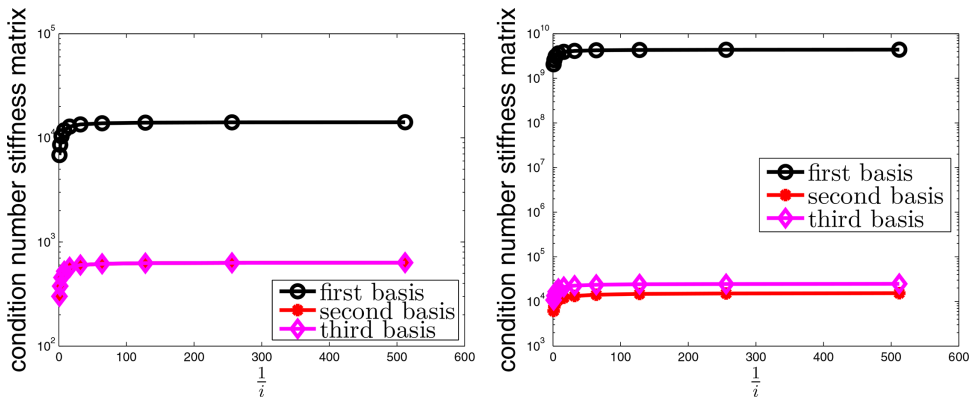


FIGURE 11 Condition numbers of the local VEM stiffness matrix on the sequence of pentagons (squares with a hanging node) depicted in Figure 10 in dependence of i , parameter used in the definition of the coordinates (38) of the pentagons K_i . The stabilization is fixed and equal to S_1^K (26). We compare the behavior in terms of the three polynomial bases presented in Section 2.3. Left: $p=3$. Right: $p=6$ [Color figure can be viewed at wileyonlinelibrary.com]

We deduce from Figures 12 and 13 again that the behaviour of the method using different stabilizations is basically the same.

4 | CONCLUSIONS

In this work, we addressed and suggested possible cures to the problem of the ill-conditioning of the virtual element method, arising from high values of the polynomial degree p and in presence of highly anisotropic elements. In particular, we focused our attention on the effects of the stabilization of the method and the choice of internal degrees of freedom. It turned out that, whereas various stabilizations

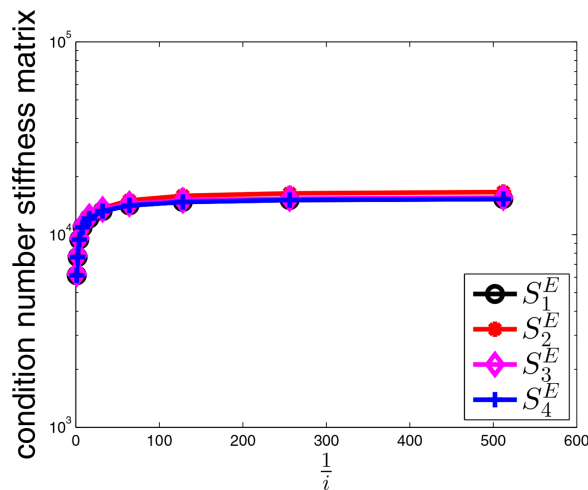


FIGURE 12 Condition numbers of the local VEM stiffness matrix on the sequence of pentagons (squares with a hanging node) depicted in Figure 10 in dependence of i , parameter used in the definition of the coordinates (38) of sequence $\{K_i\}_{i \in \mathbb{N}}$. The polynomial basis, dual to the internal moments (5) is fixed to be $\{q_\alpha^2\}_{|\alpha|=0}^{p-2}$. We compare the behavior in terms of the four stabilizations presented in Section 2.2. The degree of accuracy is $p=6$ [Color figure can be viewed at wileyonlinelibrary.com]

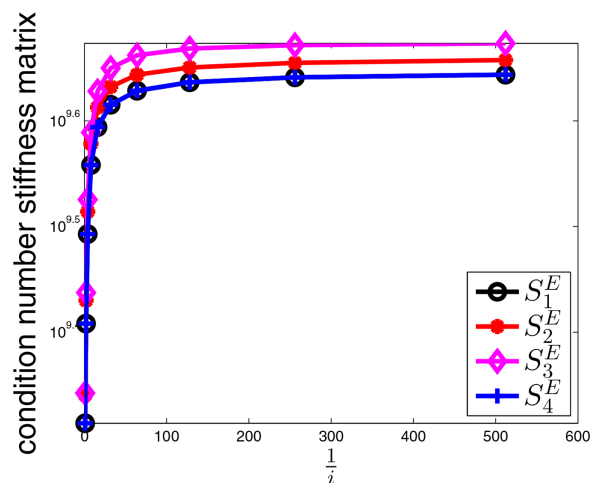


FIGURE 13 Condition numbers of the local VEM stiffness matrix on the sequence of pentagons (squares with a hanging node) depicted in Figure 10 in dependence of i , parameter used in the definition of the coordinates (38) of sequence $\{K_i\}_{i \in \mathbb{N}}$. The polynomial basis, dual to the internal moments (5) is fixed to be $\{q_\alpha^1\}_{|\alpha|=0}^{p-2}$. We compare the behavior in terms of the four stabilizations presented in Section 2.2. The degree of accuracy is $p=6$ [Color figure can be viewed at wileyonlinelibrary.com]

presented in literature have almost the same effect on the condition number of the stiffness matrix, the choice of the internal degrees of freedom has a deep impact.

We suggested two practical modifications of such internal degrees of freedom which greatly improve the behaviour of high-order VEM and VEM in presence of badly-shaped polygons.

It is worth to mention that we focused our attention to a simple 2D Poisson problem only. If one turns for instance to 3D problems, then the choice of stabilization (14) plays a major role, as shown in [33, 15].

ACKNOWLEDGMENTS

The author acknowledges the support of the Austrian Science Fund (FWF) project F 65.

ORCID

Lorenzo Mascotto  <http://orcid.org/0000-0003-3401-6652>

REFERENCES

- [1] L. Beirão da Veiga, K. Lipnikov, G. Manzini, *The mimetic finite difference method for elliptic problems*, vol. 11, Springer, Berlin, Germany, 2014.
- [2] F. Brezzi, K. Lipnikov, M. Shashkov, *Convergence of the mimetic finite difference method for diffusion problems on polyhedral meshes*, SIAM J. Numer. Anal. vol. 43 (2005) pp. 1872–1896.
- [3] P. F. Antonietti, A. Cangiani, J. Collis, Z. Dong, E. H. Georgoulis, S. Giani, P. Houston, *Review of discontinuous Galerkin finite element methods for partial differential equations on complicated domains*, in *building bridges: Connections and challenges in modern approaches to numerical partial differential equations*, Springer, Berlin, Germany, pp. 279–308, 2016.
- [4] A. Cangiani, E. H. Georgoulis, P. Houston, *hp-version discontinuous Galerkin methods on polygonal and polyhedral meshes*, Math. Models Methods Appl. Sci. vol. 24 (2014) pp. 2009–2041.

- [5] D. A. Di Pietro, A. Ern, *Hybrid high-order methods for variable-diffusion problems on general meshes*, C. R. Math. Acad. Sci. Paris, vol. 353 (2015) pp. 31–34.
- [6] B. Cockburn, B. Dong, J. Guzmán, *A superconvergent LDG-hybridizable Galerkin method for second-order elliptic problems*, Math. Comp. vol. 77 (2008) pp. 1887–1916.
- [7] J. Wang, X. Ye, *A weak Galerkin finite element method for second-order elliptic problems*, J. Comput. Appl. Math. vol. 241 (2013) pp. 103–115.
- [8] S. Rjasanow, S. Weißer, *Higher order BEM-based FEM on polygonal meshes*, SIAM J. Numer. Anal. vol. 50 (2012) pp. 2357–2378.
- [9] N. Sukumar, A. Tabarraei, *Conforming polygonal finite elements*, Internat. J. Numer. Methods Eng. vol. 61 (2004) pp. 2045–2066.
- [10] L. Beirão da Veiga, F. Brezzi, A. Cangiani, G. Manzini, L. Marini, A. Russo, *Basic principles of virtual element methods*, Math. Models Methods Appl. Sci. vol. 23 (2013) pp. 199–214.
- [11] L. Beirão da Veiga, A. Chernov, L. Mascotto, A. Russo, *Basic principles of hp virtual elements on quasiuniform meshes*, Math. Models Methods Appl. Sci. vol. 26 (2016) pp. 1567–1598.
- [12] L. Beirão da Veiga, A. Chernov, L. Mascotto, A. Russo, *Exponential convergence of the hp virtual element method with corner singularity*, Numer Math. vol. 138 (2018) pp. 581–613.
- [13] P. F. Antonietti, L. Mascotto, M. Verani, *A multigrid algorithm for the p-version of the virtual element method*, ESAIM Math. Model. Numer. Anal. (2018). In press. <https://arxiv.org/abs/1703.02285>
- [14] A. Chernov, L. Mascotto, *The harmonic virtual element method: Stabilization and exponential convergence for the Laplace problem on polygonal domains*, In press. <https://arxiv.org/abs/1705.10049>.
- [15] F. Dassi, L. Mascotto, *Exploring high-order three dimensional virtual elements: bases and stabilizations*, Comput. Math. Appl. (2018). In press. doi: <https://doi.org/10.1016/j.camwa.2018.02.005>.
- [16] L. Mascotto, I. Perugia, A. Pichler, *Non-conforming harmonic virtual element method: h- and p-versions*, In press. <https://arxiv.org/abs/1801.00578>.
- [17] G. Vacca, L. Beirão da Veiga, *Virtual element methods for parabolic problems on polygonal meshes*, Numer. Methods Partial Differential Equations, vol. 31 (2015) pp. 2110–2134.
- [18] P. F. Antonietti, L. Beirão da Veiga, S. Scacchi, M. Verani, *A C^1 virtual element method for the Cahn–Hilliard equation with polygonal meshes*, SIAM J. Numer. Anal., vol. 54 (2016) pp. 34–56.
- [19] L. Beirão da Veiga, C. Lovadina, G. Vacca, *Divergence free virtual elements for the Stokes problem on polygonal meshes*, ESAIM Math. Model. Numer. Anal. vol. 51 (2017) pp. 509–535.
- [20] I. Perugia, P. Pietra, A. Russo, *A plane wave virtual element method for the Helmholtz problem*, ESAIM Math. Model. Numer. Anal. vol. 50 (2016) pp. 783–808.
- [21] L. Beirão da Veiga, C. Lovadina, G. Vacca, *Virtual elements for the Navier–Stokes problem on polygonal meshes*, In press. arXiv:1703.00437.
- [22] P. F. Antonietti, L. Beirão da Veiga, D. Mora, M. Verani, *A stream virtual element formulation of the Stokes problem on polygonal meshes*, SIAM J. Numer. Anal. vol. 52 (2014) pp. 386–404.
- [23] L. Beirão da Veiga, C. Lovadina, D. Mora, *A virtual element method for elastic and inelastic problems on polytope meshes*, Comput. Methods Appl. Mech. Engrg. vol. 295 (2015) pp. 327–346.
- [24] L. Beirão da Veiga, F. Brezzi, L. Marini, *Virtual elements for linear elasticity problems*, SIAM J. Numer. Anal. vol. 51 (2013) pp. 794–812.
- [25] A. Gain, C. Talischi, G. Paulino, *On the virtual element method for three-dimensional elasticity problems on arbitrary polyhedral meshes*, Comput. Methods Appl. Mech. Eng. vol. 282 (2014) pp. 132–160.
- [26] L. Beirão da Veiga, F. Brezzi, L. D. Marini, A. Russo, *Mixed virtual element methods for general second order elliptic problems on polygonal meshes*, ESAIM Math. Model. Numer. Anal. vol. 50 (2016) pp. 727–747.
- [27] M. Frittelli, I. Sgura, *Virtual element method for the Laplace Beltrami equation on surfaces*, ESAIM Math. Model. Numer. Anal. (2017). doi: <https://doi.org/10.1051/m2an/2017040>.
- [28] S. Bertoluzza, M. Pennacchio, D. Prada, *BDDC and FETI-DP for the virtual element method*, Calcolo vol. 54 (2013) pp. 1565–1593.

- [29] M. Benedetto, S. Berrone, S. Scialò, *A globally conforming method for solving flow in discrete fracture networks using the virtual element method*, *Finite Elem. Anal. Des.* vol. 109 (2016) pp. 23–36.
- [30] L. Beirão da Veiga, F. Brezzi, L. D. Marini, A. Russo, *Serendipity nodal VEM spaces*, *Comput. Fluids* vol. 141 (2016) pp. 2–12.
- [31] L. Beirão da Veiga, F. Brezzi, L. Marini, A. Russo, *The hitchhiker's guide to the virtual element method*, *Math. Models Methods Appl. Sci.* vol. 24 (2014) pp. 1541–1573.
- [32] B. Ahmad, A. Alsaedi, F. Brezzi, L. Marini, A. Russo, *Equivalent projectors for virtual element methods*, *Comput. Math. Appl.* vol. 66 (2013) pp. 376–391.
- [33] L. Beirão da Veiga, F. Dassi, A. Russo, *High-order virtual element method on polyhedral meshes*, *Comput. Math. Appl.* vol. 74 (2017) pp. 1110–1122.
- [34] S. Berrone, A. Borio, *Orthogonal polynomials in badly shaped polygonal elements for the virtual element method*, *Finite Elem. Anal. Des.* vol. 129 (2017) pp. 14–31.
- [35] C. Schwab, *p- and hp- finite element methods: Theory and applications in solid and fluid mechanics*, Clarendon Press Oxford, 1998.
- [36] M. Dubiner, *Spectral methods on triangles and other domains*, *J. Sci. Comput.* vol. 6 (1991) pp. 345–390.
- [37] S. Adjerid, M. Aiffa, J. Flaherty, *Hierarchical finite element bases for triangular and tetrahedral elements*, *Comput. Methods Appl. Mech. Eng.* vol. 190 (2001) pp. 2925–2941.
- [38] L. C. Evans, *Partial differential equations*, American Mathematical Society, Providence, Rhode Island, 2010.
- [39] R. A. Adams, J. J. F. Fournier, *Sobolev Spaces*, vol. 140, Academic Press, Cambridge, MA, 2003.
- [40] S. C. Brenner, L. R. Scott, *The mathematical theory of finite element methods*, vol. 15, 3rd edn., Texts in Applied Mathematics, Springer-Verlag, New York, 2008.
- [41] L. Beirão da Veiga, C. Lovadina, A. Russo, *Stability analysis for the virtual element method*, *Math. Models Methods Appl. Sci.* vol. 27 (2017) pp. 2557–2594.
- [42] F. Bassi, L. Botti, A. Colombo, D. A. Di Pietro, P. Tesini, *On the flexibility of agglomeration based physical space discontinuous Galerkin discretizations*, *J. Comput. Phys.* vol. 231 (2012) pp. 45–65.
- [43] R. Pasquetti, F. Rapetti, *Spectral element methods on triangles and quadrilaterals: Comparisons and applications*, *J. Comput. Phys.* vol. 198 (2004) pp. 349–362.
- [44] C. Canuto, M. Y. Hussaini, A. Quarteroni, T. A. Zhang, *Spectral methods in fluid dynamics*, Springer Science & Business Media, Berlin, Germany, 2012.

How to cite this article: Mascotto L. Ill-conditioning in the virtual element method: Stabilizations and bases. *Numer. Methods Partial Differential Eq.* 2018;34:1258–1281. <https://doi.org/10.1002/num.22257>

APPENDIX A: A HITCHHIKERS GUIDE FOR THE IMPLEMENTATION OF VEM USING BASIS $\{q_\alpha^2\}_{|\alpha|=0}^{p-2}$

We discuss here the implementation details for the construction of the method employing basis $\{q_\alpha^2\}_{|\alpha|=0}^{p-2}$ as a dual basis for the internal moments (5). Henceforth, we adopt the notation of Section 2.3. Moreover, given a matrix $\mathbf{A} \in \mathbb{R}^{n \times m}$, we will denote by:

$$\mathbf{A}(i : j, \ell : k),$$

the submatrix of \mathbf{A} from row i to j and from column ℓ to k .

Let us define by $\{q_\alpha^2\}_{|\alpha|=0}^p$ the basis of $\mathbb{P}_p(K)$ obtained by an L^2 orthonormalization of basis $\{q_\alpha^1\}_{|\alpha|=0}^{p-2}$ using the stable Gram-Schmidt process presented in [42]. In particular, we can write (always using

with a little abuse of notation the bijection [30]):

$$q_\alpha^2(\mathbf{x}) = \sum_{\beta=1}^{\alpha} \mathbf{GS}_{\alpha,\beta} q_\beta^1(\mathbf{x}) \quad \forall \alpha \in \mathbb{N}^2, \quad |\alpha| = 0, \dots, p,$$

where \mathbf{GS} is the lower triangular matrix containing the orthonormalizing coefficients.

In [31], the implementation details employing basis $\{q_\alpha^1\}_{|\alpha|=0}^{p-2}$ defined in (31) were discussed. In particular, it was proven that the local stiffness matrix was defined through some auxiliary matrices which we recall here:

$$\begin{aligned} 20 \mathbf{G}_{\alpha,\beta} &= \begin{cases} P_0(q_\beta^1) & \text{if } \alpha = 1 \\ (\nabla q_\alpha^1, \nabla q_\beta^1)_{0,K} & \text{if } \alpha \geq 2 \end{cases}, & \tilde{\mathbf{G}}_{\alpha,\beta} &= (\nabla q_\alpha^1, \nabla q_\beta^1)_{0,K}, \\ \mathbf{D}_{j,\alpha} &= \text{dof}_j^1(q_\alpha^1), & \mathbf{B}_{a,j} &= \begin{cases} P_0 \varphi_j^1 & \text{if } \alpha = 1 \\ (\nabla q_\alpha^1, \nabla \varphi_j^1)_{0,K} & \text{if } \alpha \geq 2 \end{cases}, \\ \forall \alpha, \beta \in \mathbb{N}^2, & |\alpha|, |\beta| = 0, \dots, p, \quad i = 0, \dots, N_{\text{dof}}^K, \end{aligned} \tag{40}$$

where P_0 is defined in (10).

The local stiffness matrix reads:

$$\mathbf{K}_p^K = (\mathbf{\Pi}_*^\nabla)^t \cdot \tilde{\mathbf{G}} \cdot (\mathbf{\Pi}_*^\nabla) + (\mathbf{Id} - \mathbf{\Pi}^\nabla)^t \cdot \mathbf{S}^K \cdot (\mathbf{Id} - \mathbf{\Pi}^\nabla), \tag{41}$$

where \mathbf{S}^K denotes the matrix associated with any of the bilinear forms S^K introduced in (14), where $\mathbf{\Pi}_*^\nabla$ denotes the matrix associated with operator Π_p^∇ introduced in (9) acting from the local VE space $V_p(K)$ to $\mathbb{P}_p(K)$ with respect to basis $\{q_\alpha^1\}_{|\alpha|=0}^{p-2}$ and where $\mathbf{\Pi}^\nabla$ denotes the matrix associated with the operator Π_p^∇ introduced in (9) acting from the local VE space $V_p(K)$ to $\mathbb{P}_p(K)$ with respect to basis $\{\varphi_j^1\}_{j=1}^{N_{\text{dof}}^K}$.

It was shown in [31] that:

$$\mathbf{\Pi}_*^\nabla = \mathbf{G}^{-1} \cdot \mathbf{B}, \quad \mathbf{\Pi}^\nabla = \mathbf{D} \cdot \mathbf{G}^{-1} \cdot \mathbf{B}.$$

The aim of this section is to write the local stiffness matrix using the new canonical basis associated with polynomial basis $\{q_\alpha^2\}_{|\alpha|=0}^{p-2}$ and expanding all the projectors with respect to the polynomial spaces on polynomial basis $\{q_\alpha^2\}_{|\alpha|=0}^p$.

For the sake of simplicity, we denote the counterpart of the VEM matrices in (40) and (41) associated with bases $\{q_\alpha^2\}_{|\alpha|=0}^p$ and $\{\varphi_j^2\}_{j=1}^{N_{\text{dof}}^K}$, with a bar at the top of each one of them.

We explain how to compute in the new setting such new matrices. We start with matrix $\overline{\tilde{\mathbf{G}}}$, which is defined as:

$$\overline{\tilde{\mathbf{G}}}_{\alpha,\beta} = (\nabla q_\alpha^2, \nabla q_\beta^2)_{0,K} \quad \forall \alpha, \beta \in \mathbb{N}^2, \quad |\alpha|, |\beta| = 0, \dots, p.$$

One simply has to compute:

$$\overline{\tilde{\mathbf{G}}} = \mathbf{GS} \cdot \tilde{\mathbf{G}} \cdot \mathbf{GS}^T.$$

Now, we consider matrix $\bar{\mathbf{G}}$ defined as:

$$\bar{\mathbf{G}}_{\alpha,\beta} = \begin{cases} P_0(q_\beta^2) & \text{if } \alpha = 1 \\ (\nabla q_\alpha^2, \nabla q_\beta^2) & \text{if } \alpha \geq 2 \end{cases} \quad \forall \alpha, \beta \in \mathbb{N}^2, \quad |\alpha|, |\beta| = 0, \dots, p,$$

where $P_0(\cdot)$ is defined in (10). We obviously have to take care only of the first line of the matrix since the remainder is inherited from $\bar{\mathbf{G}}$. We distinguish two cases.

($p = 1$) $P_0(q_\beta^2) = \frac{1}{N_K} \sum_{\ell=1}^{N_K} q_\beta^2(v_\ell)$, where we recall that v_ℓ is the ℓ -th vertex of K . We shall then write:

$$\begin{aligned} P_0(q_\beta^2) &= \frac{1}{N_K} \sum_{\ell=1}^{N_K} \left(\sum_{\gamma \leq \beta} \mathbf{GS}_{\beta,\gamma} q_\gamma^1(v_\ell) \right) = \sum_{\gamma=1}^{\beta} \mathbf{GS}_{\beta,\gamma} \left(\frac{1}{N_K} \sum_{\ell=1}^{N_K} q_\gamma^1(v_\ell) \right) \\ &= \sum_{\gamma=1}^{\beta} \mathbf{GS}_{\beta,\gamma} \mathbf{G}_{1,\gamma} = \mathbf{GS}(\beta, 1 : \beta) \cdot \mathbf{G}(1, 1 : \beta)^T. \end{aligned}$$

($p \geq 2$) In this case, we have:

$$P_0(q_\beta^2) = \frac{1}{|K|} \int_K q_\beta^2 = \mathbf{GS}_{1,1}^{-1} \frac{1}{|K|} \int_K q_\beta^2 \mathbf{GS}_{1,1} = \mathbf{GS}_{1,1}^{-1} \frac{1}{|K|} \int_K q_1^2 q_\beta^2 = \begin{cases} \frac{1}{\mathbf{GS}_{1,1} |K|} & \text{if } \beta = 1 \\ 0 & \text{else} \end{cases},$$

as basis $\{q_\alpha^2\}_{\alpha=1}^{n_p}$ is $L^2(K)$ orthonormal by construction.

Next, we turn our attention to matrix $\bar{\mathbf{D}}$ which is defined as:

$$\bar{\mathbf{D}}_{j,\alpha} = \text{dof}_j^2(q_\alpha^2) \quad \forall \alpha \in \mathbb{N}^2, \quad |\alpha| = 0, \dots, p, \quad j = 1, \dots, N_{\text{dof}}^K$$

and we distinguish two situations.

- Let us consider firstly the boundary dofs:

$$\bar{\mathbf{D}}_{j,\alpha} = \text{dof}_j^2(q_\alpha^2) = q_\alpha^2(\xi_j) = \sum_{\beta=1}^{\alpha} \mathbf{GS}_{\alpha,\beta} q_\beta^1(\xi_j) = \sum_{\beta=1}^{\alpha} \mathbf{GS}_{\alpha,\beta} \mathbf{D}_{j,\beta} = \mathbf{GS}(\alpha, 1 : \alpha) \cdot \mathbf{D}(j, 1 : \alpha)^T.$$

where ξ_j is a proper node on the boundary.

- Next, we deal with the internal dofs. One simply has, if q_γ^2 is the polynomial associated with dof_j:

$$\text{dof}_j^2(q_\alpha^2) = \frac{1}{|K|} \int_K q_\alpha^2 q_\gamma^2 = \frac{1}{|K|} \delta_{\alpha,j} \quad \forall j = 1, \dots, n_{p-2},$$

owing again to the L^2 orthonormality of basis $\{q_\alpha^2\}_{|\alpha|=0}^p$.

Finally, we discuss the construction of matrix $\bar{\mathbf{B}}$ which is defined as:

$$\bar{\mathbf{B}}_{\alpha,j} = \begin{cases} P_0(\varphi_j^2) & \text{if } \alpha = 1 \\ (\nabla q_\alpha^2, \nabla \varphi_j^2) & \text{if } \alpha \geq 2 \end{cases} \quad \forall \alpha \in \mathbb{N}^2, \quad |\alpha| = 0, \dots, p, \quad \forall j = 1, \dots, N_{\text{dof}}^K.$$

We first, deal with the first line and we consider the two cases $p = 1$ and $p \geq 2$.

($p = 1$) $P_0(\varphi_j^2) = \frac{1}{N_K} \sum_{\ell=1}^{N_K} \varphi_j^2(v_\ell) = \frac{1}{N_K} \sum_{\ell=1}^{N_K} \varphi_j^1(v_\ell)$, where we recall that $\{v_\ell\}_{\ell=1}^{N_K}$ is the set of vertices of polygon K . Thus $\bar{\mathbf{B}}_{1,j} = \mathbf{B}_{1,j} \forall j = 1, \dots, N_{\text{dof}}^K$.

($p \geq 2$) In this case, we can write:

$$\begin{aligned} P_0(\varphi_j^2) &= \frac{1}{|K|} \int_K \varphi_j^2 = \mathbf{GS}_{1,1}^{-1} \frac{1}{|K|} \int_K \varphi_j^2 \mathbf{GS}_{1,1} = \mathbf{GS}_{1,1}^{-1} \frac{1}{|K|} \int_K \varphi_j^2 q_1^2 \\ &= \begin{cases} \mathbf{GS}_{1,1}^{-1} & \text{if } \varphi_j \text{ is the first internal element,} \\ 0 & \text{else,} \end{cases} \end{aligned}$$

as $q_1^2 = \mathbf{GS}_{1,1} q_1^1 = \mathbf{GS}_{1,1}$. Thus $\bar{\mathbf{B}}_{1,j} = \mathbf{GS}_{1,1}^{-1} \mathbf{B}_{1,j} \forall j = 1, \dots, N_{\text{dof}}^K$.

Next, we treat all the other lines. We must compute $(\nabla q_\alpha^2, \nabla \varphi_j^2)_{0,K}$. Again, we consider two different situations.

- If φ_j^2 is a boundary basis function, that is, $j = 1, \dots, pN_K$, where we recall that N_K is the number of edges (and vertices) of K , then:

$$\begin{aligned} (\nabla q_\alpha^2, \nabla \varphi_j^2)_{0,K} &= \int_{\partial K} (\partial_n q_\alpha^2) \varphi_j^2 = \sum_{\beta=1}^\alpha \mathbf{GS}_{\alpha,\beta} \int_{\partial K} (\partial_n q_\beta^1) \varphi_j^2 \\ &= \sum_{\beta=1}^\alpha \mathbf{GS}_{\alpha,\beta} \int_{\partial K} (\partial_n q_\beta^1) \varphi_j^1 = \sum_{\beta=1}^\alpha \mathbf{GS}_{\alpha,\beta} \mathbf{B}_{\beta,j} = \mathbf{GS}(\alpha, 1 : \alpha) \cdot \mathbf{B}(1 : \alpha, j), \end{aligned}$$

where we used that it holds $\varphi_j^1|_{\partial K} = \varphi_j^2|_{\partial K}$.

- Assume now φ_j^2 is an internal basis function. This case is a bit more involved. We write:

$$(\nabla q_\alpha^2, \nabla \varphi_j^2)_{0,K} = - \int_K (\Delta q_\alpha^2) \varphi_j^2. \tag{42}$$

We expand Δq_α^2 into a combination of elements of the basis $\{q_\beta^2\}_{\beta=0}^{p-2}$, since the Laplace operator eliminates the high ($p - 1$ and p) polynomial degree contributions. We get:

$$\Delta q_\alpha^2 = \sum_{|\beta|=0}^{p-2} \bar{\mathbf{F}}_{\alpha,\beta} q_\beta^2. \tag{43}$$

We only need to compute the entries of matrix $\bar{\mathbf{F}}$. For the purpose, we test (43) with q_γ^2 thus obtaining:

$$\bar{\mathbf{F}}_{\alpha,\gamma} = (\Delta q_\alpha^2, q_\gamma^2)_{0,K} = -(\nabla q_\alpha^2, \nabla q_\gamma^2)_{0,K} + (\partial_n q_\alpha^2, q_\gamma^2)_{0,\partial K}.$$

The first term is nothing but $-\bar{\mathbf{G}}_{\alpha,\gamma}$. We wonder how to compute the second term. We note that matrix \mathbf{L} defined as:

$$\mathbf{L}_{\alpha,\beta} = \int_{\partial K} (\partial_n q_\alpha^1) q_\beta^1 \quad \forall \alpha, \beta \in \mathbb{N}^2, \quad |\alpha|, |\beta| = 0, \dots, p,$$

can be computed exactly. For the sake of completeness, we explicitly write how. Given $\mathcal{E}(K)$ the set of edges of K :

$$\mathbf{L}_{\alpha,\beta} = \sum_{e \in \mathcal{E}(K)} \int_e (\partial_n q_\alpha^1) q_\beta^1 = \sum_{e \in \mathcal{E}(K)} \left\{ \sum_{k=0}^p \omega_k^e ((\partial_n q_\alpha^1) q_\beta^1) (v_k^e) \right\},$$

where ω_k^e and v_k^e , $k = 0, \dots, p$, are the k -th weights and nodes of the Gauß-Lobatto quadrature over edge e . It is easy to check that if we set:

$$\bar{\mathbf{L}}_{\alpha,\beta} = \int_{\partial K} (\partial_n q_\alpha^2) q_\beta^2,$$

then:

$$\bar{\mathbf{L}} = \mathbf{GS} \cdot \mathbf{L} \cdot \mathbf{GS}^T.$$

As a consequence:

$$\bar{\mathbf{F}} = \bar{\mathbf{L}} - \bar{\mathbf{G}}.$$

Now, we plug (43) in (42) obtaining:

$$\bar{\mathbf{B}}_{\alpha,j} = (\nabla q_\alpha^2, \nabla \varphi_j^2) = - \sum_{\beta=1}^{n_{p-2}} \bar{\mathbf{F}}_{\alpha,\beta} (q_\beta^2, \varphi_j^2)_{0,K} = - \sum_{\beta=1}^{n_{p-2}} \bar{\mathbf{F}}_{\alpha,\beta} \bar{\mathbf{C}}_{\beta,j} = -\bar{\mathbf{F}}(\alpha, 1 : n_{p-2}) \cdot \bar{\mathbf{C}}(1 : n_{p-2}, j),$$

where $\bar{\mathbf{C}}$ is a matrix defined as follows:

$$\bar{\mathbf{C}}_{\alpha,j} = (q_\alpha^2, \varphi_j^2)_{0,K} \quad \forall \alpha \in \mathbb{N}^2, \quad |\alpha| = 0, \dots, p-2, \quad \forall j = 1, \dots, N_{\text{dof}}^K.$$

One has:

$$(q_\alpha^2, \varphi_j^2)_{0,K} = \begin{cases} 0 & \text{if } \varphi_j^2 \text{ is a boundary basis element} \\ |K| \frac{1}{|K|} \int_K q_\alpha^2 \varphi_j^2 = \delta_{\alpha,j} |K| & \text{otherwise} \end{cases}.$$